

This discussion paper is/has been under review for the journal Solid Earth (SE).
Please refer to the corresponding final paper in SE if available.

High-grade deformation in quartzo-feldspathic gneisses during the early Variscan exhumation of the Cabo Ortegal nappe, NW of Iberia

F. J. Fernández¹, S. Llana-Fúnez¹, A. Marcos¹, P. Castiñeiras², and P. Valverde-Vaquero³

¹Departamento de Geología, Universidad de Oviedo, Jesús Arias de Velasco s/n, 33005 Oviedo, Spain

²Departamento de Petrología y Geoquímica, Universidad Complutense de Madrid, José Antonio Novais 12, 28040 Madrid, Spain

³Área de laboratorios, Instituto Geológico y Minero de España, La Calera 1, 28760 Tres Cantos, Spain

Received: 25 November 2015 – Accepted: 1 December 2015 – Published: 7 December 2015

Correspondence to: F. J. Fernández (brojos@geol.uniovi.es)

Published by Copernicus Publications on behalf of the European Geosciences Union.

3541

Abstract

High-grade highly deformed gneisses crop out continuously along the Masanteo peninsula in the Cabo Ortegal nappe (NW Spain). The rock sequence formed by quartzo-feldspathic gneisses and mafic rocks records two partial melting events: during the
5 Early Ordovician (ca. 480–488 Ma.), at the base of the Qz-Fsp gneisses, and immediately after eclogization (ca. 390.4 ± 1.2 Ma), during its early Variscan exhumation. Despite the strain accumulated during their final exhumation in which a pervasive blastomylonitic S_2 foliation was developed, primary sedimentary layering in Qz-Fsp gneisses is well preserved locally at the top of the sequence. This first stage of the exhumation
10 process occurred in ~ 10 Ma, during which bulk flattening of the high-grade rock sequence was accommodated by anastomosing shear bands that evolved to planar shear zones. Strain was progressively localized along the boundaries of the migmatitic Qz-Fsp gneisses. A SE-vergent ductile thrust constitutes the base of gneisses, incorporating eclogite blocks-in-matrix. A NW-vergent detachment placed the metasedimentary
15 Qz-Fsp gneisses over the migmatitic Qz-Fsp gneisses. A difference in metamorphic pressure of ca. 0.5 GPa is estimated between both gneissic units. The high-grade deformation reduced substantially the thickness of the gneissic rock sequence during the process of exhumation controlled by change in the strain direction and the progressive localization of strain. The combined movement of the top detachment and basal
20 thrust resulted in an extrusion of the migmatites within the nappe, directed to the SE in current coordinates.

1 Introduction

The processes involved in the exhumation of HP and UHP rocks in subduction zones remain a hot topic in tectonics given the complexity of strain paths that rocks follow
25 from the surface to great depths and back to the surface (e.g. Gerya and Stöckhert, 2006). The boundary between convergent plates concentrates a large amount of strain

3542

and also heterogeneity. This boundary in subduction zones, named as the subduction channel, is characterized by non-parallel planar rigid edges on either side, on profile having a triangular shape (i.e. Bird, 1978; England and Holland, 1979; Shreve and Cloos, 1986; Mancktelow, 1995). Under this configuration, the convergence of rigid plates squeezing a non-compressible viscous material, introduces a stress gradient in the system leading to lateral flow of rock (e.g. Mancktelow, 1995). If the shearing associated to the convergence is taken into account, the result is that particles close to the subducting plate will follow the lower boundary and once they reach the vortex of the triangular channel will return to the surface following the upper rigid boundary (see Fig. 4 in Shreve and Cloos, 1986). The intrinsic heterogeneity of the system at the boundary between plates can be now visualised in numerical models, however, the rock record does not always preserve all deformation stages and the difficulty in interpreting a finite strain path in rocks and rock units remains.

In continental collision, subsequent in most cases to a subduction stage, there are some analogies with the “subduction channel” or the boundary between plates, but some major differences. The first major difference is that as a consequence of less rigid plate boundaries involved the size of this idealized triangular plate boundary increases substantially. It is renamed as an orogenic wedge or an accretionary wedge. It has a triangular shape, but the angles between sides change. Displacement paths of particles within the system do follow the sides of this wedge, but the dynamics are completely different. In orogenic wedges, the exhumation of subducted rocks from depth greater than 50 km cannot be satisfactorily explain by classical collision models, such as the dynamics of accretionary wedge (i.e. Davis et al., 1983; Platt, 1986) or the extensional exhumation (i.e. Chemenda et al., 1995).

Extrusion of high-grade rocks is usually related to the dynamics of channel flow at crustal scale in collisional orogens, in which flow of a weak lower-crustal layer towards the orogenic foreland is consequence of the collision. In the case of the Himalayan-Tibet system, the excessive crustal thickness beneath the Tibetan Plateau determines the anomalous lithostatic pressure gradient required to force lateral and frontal flow of

3543

a ductile lower crust (e.g. Beaumont et al., 2004; Rutter et al., 2011). Highly sheared migmatized rock of the Greater Himalayan sequence between the Main Central thrust and the South Tibetan detachment are effectively extruding towards the foreland.

In fact nowadays, insights from numerical models of UHP exhumation at the continental phase are consistent with a multi-stage process, where exhumation seems to start after continental subduction for most continental collision zones (e.g. Burov et al., 2014a, b).

Relics of the plate boundary between northern Gondwana and an accretionary complex and Laurasia are preserved in the high-grade allochthonous complexes of NW Iberia (e.g. Ries and Shackleton, 1971; Martínez-Catalán et al., 1997; Matte, 2001). The aims of this study, taking advantage of excellent exposure conditions of high grade structures in the Cabo Ortegal Complex, are to show in detail the architecture of a tectonic sequence composed of mafic and quartzo-feldspatic gneisses and discuss the tectonic evolution based on the structural relationships and the insights of recent U-Pb ages. The deformation features of some well-preserved high-grade structures in the field might be key to understand the processes of orogenic collision as well as to constrain thermo-mechanical models.

2 The geological framework: the Cabo Ortegal Complex

High-grade relicts of continental collision tectonically overlie most of the hinterland of the Variscan orogeny in NW Iberia forming a tectonic pile of oceanic and sedimentary material that can be recognized totally or partially within five allochthonous complexes (Martínez-Catalán et al., 1997). Three units form the orogenic tectonic pile. The upper unit is composed of ultrabasic, mafic and quartzo-feldspatic rocks that recorded high pressure and high temperature (HP-HT) metamorphism (e.g. Vogel, 1967). Rocks of distinct geodynamic settings, such as E-MORB basalts, tectonic melanges and calc-alkaline arc volcanics (Arenas, 1986; Díaz-García et al., 1999; Arenas et al., 2007) form the intermediate ophiolitic unit. The basal unit is formed by metasediments intruded by

3544

acid and basic calc-alkaline igneous rocks that recorded blueschist facies and eclogite facies conditions (Gil-Ibarguchi and Ortega-Girones, 1985; Arenas et al., 1995; López-Carmona et al., 2010, 2014).

The Cabo Ortegal complex is the allochthonous terrane located closer to the fore-
5 land basin (Fig. 1a). Internally is further divided into two tectonic units, the Cabo Ortegal
nappe and the lower unit (Marcos et al., 2002). The Cabo Ortegal nappe (Fig. 1b) is
composed of rocks affected by HP-HT metamorphism and it correlates with the upper
units of the orogenic tectonic pile. The Lower tectonic unit is composed of three thrust
10 sheets that correlate with the ophiolitic and the basal units in the other allochthonous
complexes. The Lower Paleozoic sequence of the relative autochthonous is sepa-
rated from the Cabo Ortegal complex by a thin thrust sheet of parautochthonous rocks
(Marcos and Farias, 1998).

Three major ordered lithological units form the Cabo Ortegal nappe (Fig. 1c).
> 600 m of alternating serpentized peridotites and pyroxenites (Girardeau et al.,
15 1989). The ultramafic rocks are in neat contact with 400 m thick mafic unit that cul-
minates with a 100–200 m thick massive eclogite (Vogel, 1967; Galán and Marcos,
1997). The top of the sequence is formed by > 600 m of quartzo-feldspatic gneisses.
In the proximity of this contact, the gneisses include decimetric to meter-scale lenses
of eclogites, other mafic rocks and calc-silicate rocks and show many evidences of
20 migmatization (Vogel, 1967; Gil-Ibarguchi et al., 1990; Fernández, 1997). A sedimentary
compositional banding consisting of metapelitic and metapsammitic interbedded
layers characterize the top of the quartzo-feldspatic gneissic sequence. Overall, the
whole lithostratigraphic sequence has been used as a proxy for the continental crust-
mantle transition (Brown et al., 2009).

25 In this paper, we present the structural analysis of a high-grade tectonic sequence in
mafic and quartzo-feldspatic gneisses, located in the East of the Cabo Ortegal nappe
(Fig. 2a). The gneisses are well exposed in the Masanteo peninsula, 4.5 km² in area.
A detailed mapping of the gneisses and the reconstruction of the rock unit geometry

3545

on the basis of the attitude of S₂ foliation is presented with the aim of understanding
the deformation environment at the plate boundary.

2.1 Tectonic evolution of Cabo Ortegal rocks

Cabo Ortegal rocks are affected by several phases and stages of deformation and
5 metamorphism. Protolith ages in mafic rocks are in the range of 520–490 Ma and
an early HP-HT metamorphic event is estimated in the range 400–390 Ma (Santos-
Zalduegui et al., 1996; Ordóñez-Casado et al., 2001; Fernández-Suárez et al., 2002).
Subsequent partial migmatization of the mafic granulites occurred in the range of 397–
390 Ma (Fernández-Suárez et al., 2007). The subsequent tectonic evolution of the
10 Cabo Ortegal nappe is constrained by an isothermal decompression *P–T* path related
to the exhumation from metamorphic conditions above 800 °C and 1.7 GPa to amphibolite
and greenschist facies (Gil-Ibarguchi et al., 1990; Fernández, 1997; Galán and
Marcos, 2000).

The evolution of structures with time and the prograde or retrograde character of
15 the metamorphism, as recorded in tectonic fabrics and related structures, allow to de-
fine five deformation phases in the Cabo Ortegal nappe that do not have a straight
correlation with the regional three deformation phases of the Variscan deformation dis-
tinguished in the autochthonous of Iberia (Matte, 1968; Marcos, 1971). Some authors
interpret inclusion trails as D₁ structures formed during the prograde path related to
20 the subduction stage (i.e. Ábalos et al., 2003), even though only the retrograde *P–T–t*
path of such fabrics has been finely determined (Gil-Ibarguchi et al., 1990; Fernán-
dez, 1997; Galán and Marcos, 2000). All rock types of the tectonic sequence show
a first pervasive blastomylonitic tectonic fabric, which occasionally is highly heteroge-
neously developed (Fernández, 1997; Marcos et al., 2002). The main tectonic fabric
25 and associated structures define a second deformation phase (D₂), thought to form
during the exhumation from high-pressure conditions. Frequently, the blastomylonitic
S₂ foliation forms networks of anastomosed shear zones and define lozenge-shaped
bodies of layered migmatitic gneisses, preserving primary fabrics (Fernández and Mar-

3546

orthogneisses (Qz + Mc + Pl + Grt + Ms + Bt) intruded by felsic diorite dykes (Qz + Pl + Grt + Hbl ± Czo) are intercalated in this unit of biotite gneisses. The migmatitic layers, also centimetric to decimetric in thickness, show a dominant planar geometry. The total thickness of the gneissic unit ranges between 50 to 200 m. Two compositional endmembers can be distinguished: biotitic Qz-Fsp gneisses (Fig. 4d) with Ky + Grt + Bt ± Hbl ± Czo ± Ilm ± Spn, and a fraction of leucocratic and mesocratic bands of 20 and 80 %, respectively, above the mafic gneisses; and banded leucocratic Qz-Fsp gneisses (Fig. 4f) with Grt + Bt ± Ky ± Czo ± Ilm ± Spn and a fraction of 80 and 20 % of leucocratic and mesocratic bands below the unit composed of metasedimentary gneisses. The difference in modal composition may relate to differences in the primary composition of the metasedimentary rocks. However, compositional differentiation can also be consequence of migmatization and/or subsequent deformation. The phyllonitic fabric of the biotitic-gneisses, including centimetric layers of restitic material (Fig. 4e) and its location overlying the mafic gneisses points to deformation in high-grade conditions.

Peak metamorphic conditions estimated for the migmatitic gneisses in the Masanteo peninsula are 720 °C and 1.5 GPa (Gil-Ibarguchi et al., 1990). Estimates of metamorphic conditions of equivalent biotite Qz-Fsp gneisses in Punta Tarroiba (location in Fig. 1b), the Chímparra gneisses (Vogel, 1967), show slight higher values of 800 °C and 1.7 GPa (Fernández, 1997) similar to conditions calculated in the eclogites (Fig. 5).

The structural relationships between the blastomylonitic S₂ foliation and the felsic diorite dyke allows to constrain the time of intrusion because S₂ foliation transposes metric folds buckling the dykes (Fig. 4a and b), evidencing that intrusion and folding of the diorite dykes occurred previously. Since the S₂ foliation shows parallelism to the migmatitic layering and bounds concordantly the eclogite block-in-matrix (Fig. 4c), migmatization occurred at the early stages of D₂ and immediately after eclogitization. Consequently, the migmatitic Qz-Fsp gneisses recorded two melting events, an early event related to the intrusion of the diorite dykes in the orthogneiss, and a second par-

3549

tial melting event that produced the migmatitic layering, which is better preserved within the less deformed lozenges bodies surrounded by anastomosing D₂ shear bands.

3.2.1 New U-Pb ID-TIMS geochronology in the migmatitic gneiss

Two separate felsic dykes (DM-2 and DM-3; Fig. 4a and b) were dated by U-Pb ID-TIMS at the IGME geochronology laboratory in Tres Cantos (Spain). Zircon and monazite were analyzed following the procedures outlined in Rubio Ordoñez et al. (2012). The zircon fractions were chemically abraded before final dissolution.

In the case of sample DM-2, two zircon and three monazite fractions were analyzed (Table 1; Fig. 6). The zircon fractions are discordant, while the three monazite fractions overlap the Concordia curve providing concordant ages at 475 Ma (M1), 478 Ma (M2) and 485 Ma (M3). These three monazite fractions are collinear and provide a lower intercept age of 384 ± 180 Ma and an upper intercept age of 479 ± 6.5 Ma. For sample DM-3, four zircon and three monazite fractions were dated (Table 1; Fig. 6). The monazite and zircon fractions Z1, Z4 and Z3 define a mixing line anchored at 480 ± 8 Ma by the concordant monazite and an upper intercept at 2.56 Ga, suggesting Proterozoic zircon inheritance. In this sample, monazite analyses were done using single crystals. Monazites M2 and M3 overlap each other and provide a concordant age of 480 ± 1 Ma (MSWD 0.44), while monazite M1 is concordant at 488 Ma, resembling the monazite from sample DM-2. These data clearly demonstrate the presence of Cambro-Ordovician (ca. 480–490 Ma) monazite in both dykes. A similar spread of Early Ordovician monazite ages, such as those in sample DM-2, was reported by Fernandez-Suarez et al. (2002) in the Cape Ortegal complex from leucosomes of the Chímparra gneiss, suggesting minor Devonian (ca. 386 Ma) overprint of Cambro-Ordovician monazite. The same authors also reported a zircon age of 487 Ma from a leucosome in the mafic granulites. Therefore we consider that the monazites provide the best estimate for the intrusion age of the felsic dykes DM-2 and DM-3, which would be bracketed by a minimum age of 480 Ma (intercepts of the discordia lines) and a maximum age of 485–488 Ma (oldest concordant monazite fractions).

3550

cating the progressive localization of deformation. The lower domain affects the mafic gneisses along a band ca. 50 m in thickness. It contains metric- and decametric-sized sheath folds with well-developed circular patterns. This type of folding is related to deformation by general shear bulk strain (Alsop and Holdsworth, 2006). The orientation of fold apical axes indicate NW-SE stretching (Fig. 10b).

The middle domain forms in biotite Qz-Fsp gneisses and includes eclogite blocks-in-matrix. Migmatitic leucosomic and restitic layers are interbedded and deformed ductilely. Metric asymmetrical folds face to the SE (Fig. 12a and c).

The upper domain contains phyllonites ~ 10 m in thickness frequently including eclogite-blocks-in matrix. The phyllonites are affected by associated structures such as shear bands, decimetric sheath folds, superposed folds and rotational complex mantle-structures (Figs. 10c and 11). Superposed shear folds show type 3 interference pattern of folding (after Ramsay, 1967) (Figs. 11 and 12). The apical axes of the some sheath folds point towards N20E, indicating maximum ductile extension along this direction.

4.3 The internal structure of the migmatitic gneisses

A group of decametric drag folds, affecting the planar blastomylonitic S_2 foliation, dominates the internal structure. The folds are tight, with low interlimb angles ($< 30^\circ$), overturned and vergent to the SE, where the outcrops only are showing the lower part of the migmatitic gneisses (Fig. 12a). They often have associated parasitic folds, and non-cylindrical horizontal hinges. Occasionally, minor folds relate to small thrusts surfaces that imbricate eclogite-block-in-matrix parallel to the blastomylonite S_2 foliation.

A Flinn diagram using the shape of eclogite-block-in-matrix within the gneisses and according to block sizes in Fig. 13 shows that most large eclogite blocks plot near to the plane strain field, while smaller eclogite bodies plot either in the constrictional or flattening fields. The long axis of eclogite bodies does not show a preferred orientation (to the right in Fig. 13).

The Early Ordovician dioritic dykes can be regarded as passive deformation markers during D_2 deformation. A complex structure has been observed in the coastal section

3553

at the Serrón beach (Fig. 12b). In this section, the thickness of the migmatitic Qz-Fsp gneisses is less than 100 m and both bottom and top boundaries of such unit are well exposed. Their thickness decreases progressively toward the SE. Migmatitic gneisses are affected by a shear zone in which the sense of the shear changes between the top and the bottom, producing folds of opposite vergence in the dioritic dykes and in the migmatitic banding. The larger structure reconstructed from both markers (dioritic dykes and migmatitic banding) consists in a opposite vergence recumbent hinge defined by the competent dioritic dykes. The limbs are disrupted and boudinaged toward the horizontal high strain zones located in both boundaries of this unit. This sandwiched structure indicates orthogonal stretching with transport flow of the migmatitic gneisses toward the SE, suggesting Poiseuille flow with maxima flow rate in the middle of the structure.

4.4 The top detachment

A horizontal discrete shear zone constituting the contact between the metasedimentary and the migmatitic gneisses is exposed at the Serrón beach (Fig. 12b and c). A gradual transition between both types of gneisses is observed along the base of the cliffs. Deformation partitions into anastomosing D_2 shear bands preserving evidences of previous melting episodes (Figs. 4e and 7a).

The horizontal shear zone has 20 m in thickness and strongly deflects the migmatitic layering. Migmatitic layering and diorite dykes are disrupted and boudinaged progressively towards the upper high-strain surface (Fig. 12c). Top to NW shear sense is inferred from the deflection of the migmatitic layering, drag folds and the boudinage of the dioritic dykes. Despite subsequent reequilibration in greenschists-facies conditions, evidencing a late reactivation, the mineral assemblages in the progressively less deformed bands within the detachment are basically the same as the high-grade Qz-Fsp gneisses described previously (Fig. 5).

4.5 The upper D₃ recumbent fold

The metasedimentary Qz-Fsp gneisses form the core of a recumbent synformal structure, towards the east of the Masanteo peninsula. This large-scale fold has associated several parasitic cylindrical-folds and a crenulation cleavage. Detailed cross-sections of the recumbent synform have been constructed using the asymmetry of small-scale parasitic folds and the structural relation between its associated crenulation cleavage and the main S₂ foliation (Fig. 14). The fold axis plunges 5–30° towards N20E. The fold attitude determines that the reverse limb is exposed in the northeastern cliffs and only partially along the southeast shoreline. A late upright antiform refolds the recumbent synform. This late folding affects the crenulation cleavage (Fig. 14c), which is equilibrated in greenschists-facies conditions.

Intrafoliar folds and sheath-folds, formed during the development of the S₂ foliation (Fig. 15c and d), are refolded by parasitic folds related to the recumbent fold (Fig. 14b). A late upright open fold (Fig. 15b and e) refolded this complex superposed folded structure, recording at least three different stages of progressive deformation. The recumbent syncline can be located into the larger scale cross-section of the Cabo Ortegal nappe (Fig. 1b; Marcos et al., 2002).

5 Metamorphic evolution in the gneisses

In the study area, there are evidences for two partial melting events that are recorded in the rock sequence. A first event is related to the intrusion of dioritic dykes in the orthogneisses intercalated within the migmatitic gneisses (Table 1; Fig. 6). The intrusives are synchronous, to the segregation of leucosome from the mafic granulites and yield Lower Ordovician ages, ca. 485 Ma (Fernández-Suárez et al., 2002). A second partial melting event in relict layers within Qz-Fsp gneisses postdates eclogitization of mafic block within the gneisses, at ca. 390 Ma, (sample COZ4 located in Figs. 2a and 12a; Castiñeiras et al., 2010).

3555

HP-HT metamorphism followed by rapid decompression has been determined for the D₂ tectonic fabric based on the M₂ metamorphic assemblages defining the main foliation in the migmatitic Qz-Fsp gneisses and eclogites (Gil-Ibarguchi et al., 1990; Fernández, 1997). The *P–T* path estimated for the metasedimentary Qz-Fsp gneisses in Fig. 5 preserves part of the prograde history before the final exhumation of the gneisses (Castiñeiras, 2005). An U-Pb cooling age of ca. 380 Ma has been inferred in both Qz-Fsp gneisses and eclogites of the Cabo Ortegal nappe (Valverde and Fernández, 1996; Ordóñez-Casado et al., 2001).

6 Discussion

6.1 Implications for the tectonic evolution

The tectono-metamorphic and geochronological imprints reported in this paper are integrated into three stages that allow to incorporate the geological observations around the Masanteo peninsula into the tectonic evolution of the Cabo Ortegal nappe (Fig. 16). The first stage is characterized by the building of a high grade tectonic sequence composed by mafic granulite and Qz-Fsp gneisses on top. The partial melting of the mafic granulites led to the intrusion of the diorite dykes into orthogneisses during the Early Ordovician (ca. 490 Ma).

A Devonian subduction is recorded in the eclogite facies metamorphism, prior to the main Variscan subduction at ca. 370 Ma. The exhumation from eclogite facies conditions is characterized by the bulk flattening of the whole tectonic sequence, during the pervasive but heterogeneous development of the blastomylonite S₂ foliation. The progressive localization of strain and changes in the bulk-strain direction is recorded in the “internal” extrusion of the migmatitic Qz-Fsp gneisses (Fig. 16b). A tectonic setting of ductile slab breakoff agrees with the significant thinning of the tectonic sequence and could have enhanced the extensive eclogitization by downdip extension of the subducting slab (Llana-Fúnez et al., 2004). Numerical models of continental subduction predict

3556

that change in the force balance after the first slab break-off might slow down or cancel continental subduction phase and trigger the initiation of the exhumation phase (i.e. Burov et al., 2014a, b).

5 The formation of a D_2 wedge within the gneisses accommodates the exhumation of the higher-grade units of the tectonic sequence relative to its upper part formed by Qz-Fsp gneisses with metasedimentary appearance, rather than representing a first order structure. Similar gneiss wedge within high-pressure terranes have been reported during the late stage exhumation of the Sambagawa HP rocks from lower to upper crustal levels (Osozawa and Wakabayashi, 2015) and during the exhumation of blue-schist 10 facies rocks of Leti Island in Indonesia (Kadarusman et al., 2010). These large-scale structures developed in a non-collisional subduction setting. However, the example of the Masanteo peninsula is a small-scale structure found in a Paleozoic orogen and formed at the early stages of HP-HT rocks exhumation from continental subduction settings.

15 The third stage is dominated by the multiphase deformation imparted during the Variscan convergence, corresponding to the formation of kilometric-scale recumbent folds, thrusts and folded by upright fold verging – SE, described in Cabo Ortegal as D_3 , D_4 and D_5 phases of deformation, respectively (Fig. 16a). This late evolution of the Cabo Ortegal nappe and its kinematics (Marcos et al., 2002) is consistent and coetaneous with the deformation recorded in the underlying autochthonous rock sequence 20 in relation to the Variscan belt (Matte, 1968; Pérez-Estaún et al., 1991).

Neither the tectonothermal nor the exhumation history of the high grade tectonic sequence in Masanteo peninsula supports models such as the obtained by Beaumont et al. (2004, 2006) for the Himalaya-Tibet orogeny and recently imported for the Masanteo area by Albert et al. (2012). The latter group of authors propose a tectono-thermal 25 model for the exhumation of the eclogite facies gneisses in the Cabo Ortegal Complex where the progressive deformation in the complex is controlled by “a UHP buoyant plume”, formed by the HP-HT tectonic pile, into the metasedimentary Qz-Fsp gneisses. However, the structural data is inconsistent with such interpretation. Cross sections re-

3557

ported in Albert et al. (2012) are not in agreement with the structures outlined in the same paper based on the real sections of the Masanteo cliffs (see Figs. 4 and 8 of Albert et al., 2012). Also, the ages proposed for the different deformational events are inconsistent with the geochronological data reported here. Firstly, the large regional 5 structures are recumbent folds (D_3) cut by thrusts (D_4) that produced the stacking of the Cedeira and Capelada units (Marcos et al., 2002) during the emplacement of the allochthonous HP-HT units (including the metasedimentary Qz-Fsp gneisses) onto the NW Iberian margin. This progressive deformation occurred after the eclogitization c.a. 390 and the subsequent development of the main S_2 foliation. Secondly, the normal 10 detachment and the ductile basal thrust described in this paper affect exclusively at the contacts between the migmatitic Qz-Fsp gneisses but not to the whole tectonic pile, which otherwise is the result of thrusting during final emplacement during the Variscan collision.

6.2 Assembly of gneisses at Masanteo: tectonic evolution

15 The tectono–metamorphic relationships of the basal ductile thrust (BDT) and the normal detachment mapped in the Masanteo peninsula indicate that both discrete mechanical contacts were active before the development of the recumbent folding that affects the sequence of gneisses. These mechanical contacts upon their development became in fact the boundaries of the migmatitic Qz-Fsp gneisses (Figs. 1b and 10c). 20 The arrangement of the bounding shear zones defines an inclined E-dipping wedge with the migmatitic Qz-Fsp gneisses in the middle.

The Qz-Fsp gneisses underwent an episode of partial melting after eclogitization (at ca. 390 Ma). Migmatitic Qz-Fsp layers are heterogeneously mylonitized along anastomosing shear bands that progressed to planar shear zones, imbricating eclogite blocks 25 during D_2 (Figs. 3a and 10a). D_2 tectonic fabrics have similar high temperature CPO patterns in migmatitic and metasedimentary Qz-Fsp gneisses (Fig. 9); the patterns in both types of gneisses are consistent with flattening during D_2 .

3558

Bulk flattening strain, inferred from the D_2 tectonic fabrics, the lozenge overall structure, the CPO patterns and the scattered orientation of the kinematic markers are indicative of the tectonic regime during deformation of the migmatitic Qz-Fsp gneisses.

The internal structure of the migmatitic Qz-Fsp gneisses, consisting in a double recumbent hinge suggests horizontal flow direction toward the SE (Fig. 12). The metric sheath folds belonging to the mafic gneisses of the BDT-lower domain are also consistent with SE-stretching (Fig. 10b). Progressive localization of strain occurred simultaneously during exhumation. Frequently, Phg phenoblasts, are aligned parallel to the S_2 foliation of the migmatitic Qz-Fsp gneisses, and are bounded by Bt flakes that enclosed small prismatic shaped Grt (Fernández, 1997). These microstructures evidence the instability of Phg under isothermal decompression and consequently at high exhumation rate. However, the exhumation $P-T$ path obtained for the migmatitic Qz-Fsp gneisses is different to the metamorphic evolution inferred for the metasedimentary Qz-Fsp gneisses (Fig. 5). The differences in metamorphic conditions between both Qz-Fsp gneisses are in agreement with the generalized migmatization of the lower Qz-Fsp gneisses sequence (Figs. 4 and 7). $P-T-t$ paths suggest the burial of the metasedimentary Qz-Fsp gneisses simultaneously to the exhumation of the migmatized Qz-Fsp gneisses and consequently the Qz-Fsp tectonic pile could be thinned. In addition, the progressive localization of strain contributed to the development of the BDT and the top detachment.

The 0.5 GPa metamorphic pressure difference between both Qz-Fsp gneisses could be indicative that metasedimentary Qz-Fsp gneisses exhumed from maxima burial depths ~ 17 km lower than the migmatitic Qz-Fsp gneisses. However, if BDT and the top detachment were active simultaneously, the internal extrusion of the migmatitic Qz-Fsp gneisses was produced by a gradient in pressure and consequently the difference in depths between metasedimentary and migmatitic Qz-Fsp gneisses could be lower and could range between 15.5 and 7.5 km, assuming an overpressure 1.1 or 2 times the lithostatic pressure (i.e. Mancktelow, 1995, 2008; Moulas et al., 2013). Nevertheless, part of the tectonic pile thinning occurred during the development of the blastomylonitic S_2 foliation (i.e. Fernández, 1997; Llana-Fúnez et al., 2004). Additional

3559

thinning could have progressed throughout the reactivation of the NW-vergent top detachment (Fig. 12b and c).

7 Conclusions

A new geological map of the Masanteo peninsula that incorporates the exposures of several gneissic bodies helps in the understanding of the tectonic evolution during the exhumation of high-grade rocks in the Cabo Ortegal Complex. A tectonic regime dominated by bulk flattening largely condensed the original rock sequence in Cabo Ortegal during deformation at HP and HT.

An early episode of Variscan exhumation produced the development of a main blastomylonitic foliation equilibrated in amphibolite facies conditions. Progressive strain localization during exhumation triggered the development of anastomosing shear bands, isolating lozenge bodies. Strain weakening during deformation in bounding shear zones prevented further pervasive deformation and retrogression in the lozenges. The geometric arrangement of ductile shear zones bounding the gneisses at separate tectonic stages during the exhumation, a basal ductile thrust and a top detachment, gave way to the movement of the migmatitic Qz-Fsp gneissic body to the SE. A clear pressure difference of 0.5 GPa between the gneisses on either side of the top shear zone has been calculated that can either be interpreted in terms of the difference in lithostatic pressure representing difference in depth (~ 17 km) or a lower difference in depth if part of the “pressure” excess is related to tectonic overpressure during the extrusion of the migmatitic gneisses. The kinematics of the gneissic body is consistent with the kinematics of subsequent progressive deformation that produced the SE-vergent recumbent syncline, the reactivation of the basal ductile thrust and the late upright bulk refolding of the tectonic sequence.

Author contributions. F. J. Fernández and A. Marcos carried out the fieldwork and mapping. S. Llana-Fúnez measured and plotted the crystallographic preferred orientation of Qz-Fsp gneisses. P. Valverde-Vaquero and P. Castiñeiras determined the ages of the diorite dykes and

3560

the eclogite sample, respectively. F. J. Fernández prepared the manuscript with contributions from all co-authors.

Acknowledgements. In 1988, F. J. Fernández initiated his research career in the Masanteo peninsula under the supervision of Alberto Marcos and aimed by Andrés Pérez-Estaún. Re-visiting the area 25 years later brings new light and some understanding to Cabo Ortegal geology. Authors thank their colleagues for continuing discussion about the tectonic evolution of Cabo Ortegal. Research funds from grants CGL2011-22728, CGL2010-14890 and CGL2011-23628/BTE by the Spanish government is acknowledged. P. Castiñeiras stay at Stanford University was funded by CSIC grant PA1002435.

References

- Ábalos, B., Puelles, P., and Gil Iburguchi, J. I.: Structural assemblage of high-pressure mantle and crustal rocks in a subduction channel (Cabo Ortegal, NW Spain), *Tectonics*, 22, 1006, doi:10.1029/2002TC001405, 2003.
- Albert, R., Arenas, R., Sánchez-Martínez, S., and Gerdes, A. The eclogite facies gneisses of the Cabo Ortegal Complex (NW Iberian Massif): tectonothermal evolution and exhumation model, *J. Iber. Geol.*, 38, 389–406, doi:10.5209/rev_JIGE.2012.v38.n2.40465, 2012.
- Alsop, G. I. and Holdsworth, R. E. Sheath folds as discriminators of bulk strain type, *J. Struct. Geol.*, 28, 1588–1606, 2006.
- Anders, E. and Grevesse, N.: Abundances of the elements: meteoritic and solar, *Geochim. Cosmochim. Ac.*, 53, 197–214, 1989.
- Arenas, R., Gil Iburguchi, J. I., González-Lodeiro, F., Klein, E., Martínez Catalán, J. R., Ortega Gironés, E., de Pablo-Maciá, J. G., and Peinado, M.: Tectonostratigraphic units in the complexes with mafic and related rocks of the NW of the Iberian Massif, *Hercynica*, 2, 87–110, 1986.
- Arenas, R., Rubio-Pascual, F. J., Díaz-García, F., and Martínez Catalán, J. R.: High-pressure micro-inclusions and development of an inverted metamorphic gradient in the Santiagoschists (Órdenes-Complex, NW Iberian Massif, Spain) – evidence of subduction and syn-collisional decompression, *J. Metamorph. Geol.*, 13, 141–164, 1995.
- Arenas, R., Martínez Catalán, J. R., Sánchez-Martínez, S., Díaz-García, F., Abati, J., Fernández-Suárez, J., Andonaegui, P., and Gómez-Barreiro, J.: Paleozoic ophiolites in the

3561

- Variscan suture of Galicia (northwest Spain): distribution, characteristics and meaning, in: 4-D Framework of Continental Crust, edited by: Hatcher, R. D. et al., *Mem. Geol. Soc. Am.*, Boulder, Colo.: Geological Society of America, 200, 425–444, 2007.
- Beaumont, C., Jamieson, R. A., Nguyen, M. H., and Medvedev, S.: Crustal channel flows: 1. Numerical models with applications to the tectonics of the Himalayan-Tibet orogeny, *J. Geophys. Res.*, 109, B06406, doi:10.1029/2003JB002809, 2004.
- Beaumont, C., Nguyen, M. H., Jamieson, R. A., and Ellis, S.: Crustal flow modes in large hot orogens, in: Channel Flow, Ductile Extrusion and Exhumation in Continental Collision Zones, edited by: Law, R. D., Searle, M. P., and Godin, L., *Geological Society of London Special Publications*, London, 268, 91–145, 2006.
- Bird, P.: Initiation of intracontinental subduction in the Himalaya, *J. Geophys. Res.*, 83, 4975–4987, 1978.
- Burov, E., Francois, T., Agard, P., Le Pourhiet, L., Meyer, B., Tirel, C., Lebedev, S., Yamato, P., and Brun, J.-P.: Rheological and geodynamic controls on the mechanisms of subduction and HP/UHP exhumation of crustal rocks during continental collision: insights from numerical models, *Tectonophysics*, 631, 212–250, 2014a.
- Burov, E., Francois, T., Yamato, P., and Wolf, S.: Mechanisms of continental subduction and exhumation of HP and UHP rocks, *Gondwana Res.*, 25, 464–493, doi:10.1016/j.gr.2012.09.010, 2014b.
- Brown, D., Llana-Fúnez, S., Carbonell, R., Alvarez-Marron, J., Marti, D., and Salisbury, M. H.: Laboratory measurements of *P* wave and *S* wave velocities across a surface analog of the continental crust-mantle boundary: Cabo Ortegal, Spain, *Earth Planet. Sc. Lett.*, 285, 27–38, doi:10.1016/j.epsl.2009.05.032, 2009.
- Castiñeiras, P.: Origen y evolución tectonothermal de las unidades de O Pino y Cariño (Complejos Alóctonos de Galicia), *Lab. Xeol. Laxe, Serie Nova Terra*, 28, A Coruña, Spain, 279 pp., 2005.
- Castiñeiras, P., Gómez-Barreiro, J., Fernández, F. J., and Aguilar, C.: Power and pitfalls of trace element geochemistry in zircon from high-temperature-high-pressure rocks: some examples from NW Spain, *Goldschmidt Conference Abstracts*, Goldschmidt Conference, Knoxville, Tennessee, USA, 13–18 June 2010, A149, 2010.
- Chemenda, A. I., Mattauer, M., Malavieille, J., and Bokun, A. N.: A mechanism for syn-collisional rock exhumation and associated normal faulting: results from physical modelling, *Earth Planet. Sc. Lett.*, 132, 225–232, 1995.

3562

- Davis, D. M., Suppe, J., and Dahlen, F. A.: Mechanics of fold-and-thrust belts and accretionary wedges, *J. Geophys. Res.*, 88, 1153–1172, 1983.
- Díaz-García, F., R. Arenas, J. R. Martínez-Catalán, J. G. del Tanago, and Dunning, G. R.: Tectonic evolution of the Careon ophiolite (northwest Spain): a remnant of oceanic lithosphere in the Variscan belt, *J. Geol.*, 107, 587–605, doi:10.1086/314368, 1999.
- England, P. C. and Holland, T. J. B.: Archimedes and the Tauern eclogites: the role of buoyancy in the preservation of exotic eclogite blocks, *Earth Planet. Sc. Lett.*, 44, 287–294, 1979.
- Fernández, F. J.: Estructuras desarrolladas en gneisses bajo condiciones de alta P y T (Gneisses de Chímparra, Cabo Ortegal, A Coruña, Galicia, España), Serie Nova Terra Laboratorio Xeolóxico de Laxe, 13, Edicios do Castro, Sada (Spain), 249 pp., 1997.
- Fernández, F. J. and Marcos, A.: Mylonitic foliation development by heterogeneous pure shear under high-grade conditions in quartzofeldspathic rocks (Chimparra Gneiss Formation, Cabo Ortegal Complex, NW Spain), in: *Basement Tectonics, Europe and other Regions*, edited by: Oncken, O., and Janssen, C., 11, 17–34, 1996.
- Fernández, F. J., Chaminé, H. I., Fonseca, P. E., Munhá, J. M., Ribeiro, A., Aller, J., Fuertes-Fuente, M., and Borges, F. S.: HT-fabrics in a garnet-bearing quartzite from western Portugal: geodynamic implication for the Iberian Variscan Belt, *Terra Nova*, 15, 96–103, 2003.
- Fernández-Suárez, J., Corfu, F., Arenas, R., Marcos, A., Martínez-Catalán, J. R., Díaz García, F., Abati, J., and Fernández, F. J.: U–Pb evidence for a polyorogenic evolution of the HP–HT units of the NW Iberian Massif, *Contrib. Mineral. Petr.*, 143, 236–253, 2002.
- Fernández-Suárez, J., Díaz García, F., Jeffries, T. E., Arenas, R., and Abati, J.: Constraints on the provenance of the uppermost allochthonous terrane of the NW Iberian Massif: inferences from detrital zircon U–Pb ages, *Terra Nova*, 15, 138–144, 2003.
- Fernández-Suárez, J., Arenas, R., Abati, J., Martínez Catalán, J. R., Whitehouse, M. J., and Jeffries, T. E.: U–Pb chronometry of polymetamorphic high-pressure granulites: an example from the allochthonous terranes of the NW Iberian Variscan belt, in: *4-D Framework of Continental Crust*, edited by: Hatcher Jr., R. D., Carlson, M. P., McBride, J. H., and Martínez Catalán, J. R., Geological Society of America, Memoir, Boulder, Colo. : Geological Society of America, 200, 469–488, 2007.
- Galán, G. and Marcos, A.: Geochemical evolution of high-pressure mafic granulites from the Bacariza formation (Cabo Ortegal Complex, NW Spain): an example of a heterogeneous lower crust, *Geol. Rundsch.*, 86, 539–555, 1997.

3563

- Galán, G. and Marcos, A.: The metamorphic evolution of the high-pressure mafic granulites of the Bacariza Formation (Cabo Ortegal Complex, Hercynian belt, northwest Spain), *Lithos*, 54, 139–171, 2000.
- Gerya, T. V. and Stöckhert, B.: Two-dimensional numerical modeling of tectonic and metamorphic histories at active continental margins, *Int. J. Earth Sci.*, 95, 250–274, 2006.
- Gibbons, W. and Moreno, T. (Eds): *The Geology of Spain*, The Geological Society, London, 2002.
- Gil Ibarra, J. I. and Ortega Gironés, E.: Petrology, structure and geotectonic implications of glaucophane-bearing eclogites and related rocks from the Malpica-Tuy (MT) unit, Galicia, northwest Spain, *Chem. Geol.*, 50, 145–162, doi:10.1016/0009-2541(85)90117-2, 1985.
- Gil Ibarra, J. I., Mendía, M. S., Girardeau, J., and Peucat, J. J.: Petrology of eclogites and clinopyroxene-garnet metabasites from the Cabo Ortegal Complex (northwestern Spain), *Lithos*, 25, 133–162, 1990.
- Girardeau, J., Gil Ibarra, J. I., and Ben Jamaa, N.: Evidence for a heterogeneous Upper Mantle in the Cabo Ortegal Complex, Spain, *Science*, 245, 1231–1233, 1989.
- Godin, L., Grujic, D., Law, R. D., and Searle, M. P.: Channel flow, ductile extrusion and exhumation in continental collision zones: an introduction, in: *Channel Flow, Ductile Extrusion and Exhumation in Continental Collision Zones*, edited by: Law, R. D., Searle, M. P., and Godin, L., Geological Society of London Special Publications, London, 268, 1–23, 2006.
- Holdaway, M. J.: Stability of andalusite and the aluminum silicate phase diagram, *Am. J. Sci.*, 271, 97–131, 1971.
- Isachsen, C. E., Coleman, D. S., and Schmitz, M.: PbMacDat program, available at: <http://www.earthtime.org> (last access: 2015), 2007.
- Kadarusman, A., Maruyama, S., Kaneko, Y., Ota, T., Ishikawa, A., Sopaheluwakan, J., and Omori, S.: World's youngest blueschist belt from Leti Island in the non-volcanic Banda outer arc of eastern Indonesia, *Gondwana Res.*, 18, 189–204, 2010.
- Law, R. D.: Crystallographic fabrics: a selective review of their applications to research in structural geology, in: *Deformation Mechanisms, Rheology and Tectonics*, edited by: Knipe, R. J. and Rutter, E. H., Geological Society of London Special Publications, London, 54, 335–352, 1990.
- López-Carmona, A., Abati, J., Reche, J.: Petrologic modeling of chloritoid-glaucophane schists from the NW Iberian Massif, *Gondwana Res.*, 17, 377–391, 2010.

3564

- López-Carmona, A., Abati, J., Pitra, P., and Lee, J. K. W. Retrogressed lawsonite blueschists from the NW Iberian Massif: P - T - t constraints from thermodynamic modelling and 40 Ar/39 Ar geochronology, *Contrib. Mineral. Petr.*, 167, 987–1007, doi:10.1007/s00410-014-0987-5, 2014.
- 5 Llana-Fúnez, S., Marcos, A., Galán, G., and Fernández, F. J.: Tectonic thinning of a crust slice at high pressure and high temperature by ductile-slab breakoff (Cabo Ortegal Complex, north-west Spain), *Geology*, 32, 453–456, 2004.
- Llana-Fúnez, S., Marcos, A., and Kunze, K.: Strain geometry in Concepenido eclogites during widespread HP deformation (Cabo Ortegal complex, NW Spain), *Tectonophysics*, 401, 198–216, doi:10.1016/j.tecto.2005.03.007, 2005.
- 10 Mainprice, D., Bascou, J., Cordier, P., and Tommasi, A.: Crystal preferred orientations of garnet: comparison between numerical simulations and electron back-scattered diffraction (EBSD) measurements in naturally deformed eclogites, *J. Struct. Geol.*, 26, 2089–2102, 2004.
- Mancktelow, N.: Nonlithostatic pressure during sediment subduction and the development and exhumation of high pressure metamorphic rocks, *J. Geophys. Res.*, 100, 571–583, 1995.
- 15 Mancktelow, N. S.: Tectonic pressure: theoretical concepts and modelled examples, *Lithos*, 103, 149–177, 2008.
- Marcos, A.: Cabalgamientos y estructuras menores asociadas originados en el transcurso de una nueva fase herciniana de deformación en el occidente de Asturias (NW de España) (NW de España), *Breviora Geológica Astúrica*, 15, 59–64, 1971.
- 20 Marcos, A. and Farias, P.: La estructura de las láminas inferiores del Complejo de Cabo Ortegal y su autóctono relativo (Galicia, NO de España), *Trabajos de Geología, Universidad de Oviedo*, 20, 201–218, 1998.
- Marcos, A. and Farias, P.: La estructura de las láminas inferiores del Complejo de Cabo Ortegal y su autóctono relativo (Galicia, NW España), *Trabajos de Geología, Universidad de Oviedo*, 21, 201–220, 1999.
- 25 Marcos, A., Marquín, J., Pérez-Estaún, A., Pulgar, J. A., and Bastida, F.: Nuevas aportaciones al conocimiento de la evolución tectonometamórfica del Complejo de Cabo Ortegal (NW de España), *Cuad. Lab. Xe.*, 7, 125–137, 1984.
- 30 Marcos, A., Farias, P., Galán, G., Fernández, F. J., and Llana-Fúnez, S.: Tectonic framework of the Cabo Ortegal Complex: a slab of lower crust exhumed in the Variscan orogen (north-western Iberian Peninsula). in: *Geological Society of America Special Paper*, vol. 364, edited

3565

- by: Martínez-Catalán, J. R., Hatcher, R. D. J., Arenas, R., and Díaz García, F., *Boulder, Colo.: Geological Society of America*, 143–162, 2002.
- Martínez Catalán, J. R., Arenas, R., Díaz-García, F., and Abati, J.: Variscan accretionary complex of Northwest Iberia: terrain correlation and succession of tectonothermal events, *Geology*, 25, 1103–1106, 1997.
- 5 Martínez Catalán, J. R., Arenas, R., Díaz-García, F., Gómez-Barreiro, J., González-Cuadra, P., Abati, J., Castiñeiras, P., Fernández-Suárez, J., Sánchez-Martínez, S., Andonaegui, P., González-Clavijo, E., Díez-Montes, A., Rubio-Pascual, F. J., and Valle-Aguado, B.: Space and time in the tectonic evolution of the northwestern Iberian Massif, implications for the Variscan belt, in: *4-D Framework of Continental Crust*, edited by: Hatcher, R. D., Carlson, M. P., McBride, J. H., and Martínez Catalán, J. R., *Geological Society of America Memoir*, Boulder, Colorado, 403–423, 2007.
- 10 Matte, P.: La Structure de la Virgation Hercynienne de Galice (Espagne): Extrait des Travaux du Laboratoire de Géologie de la Faculté des Sciences de Grenoble, v. 44, Grenoble, 128 pp., 1968.
- 15 Matte, P.: The Variscan collage and orogeny (480–290 Ma) and the tectonic definition of the Armorica microplate: a review, *Terra Nova*, 13, 122–128, 2001.
- Mendia, M. S.: Petrología de la Unidad Eclogítica del Complejo de Cabo Ortegal (NW de España), *Lab. Xeol. Laxe, Serie Nova Terra*, 16, A Coruña, Spain, 424 pp., 2000.
- 20 Moulas, E., Podladchikov, Y. Y., Aranovich, L. Y., and Kostopoulos, D.: The problem of depth in geology: when pressure does not translate into depth, *Petrology*, 21, 527–538, 2013.
- Ordóñez-Casado, B., Gebauer, D., Schäfer, H. J., Gil Ibaguchi, J. I., and Peucat, J. J.: A single Devonian subduction event for the HP/HT metamorphism of the Cabo Ortegal complex within the Iberian Massif, *Tectonophysics*, 332, 359–385, 2001.
- 25 Osozawa, S. and Wakabayashi, J.: Late stage exhumation of HP metamorphic rocks, progressive localization of strain, and changes in transport direction, Sambagawa belt, Japan, *J. Struct. Geol.*, 75, 1–16, 2015.
- Parga-Pondal, I., Vegas, R., and Marcos, A.: Mapa Xeolóxico do Macizo Hespérico, in: *Publicacións da Área de Xeoloxía e Minería, Seminario de Estudos Galegos*, A Coruña, Spain, 1982.
- 30 Peucat, J. J., Bernard-Griffiths, J., Gil Ibaguchi, J. I., Dallmeyer, R. D., Menot, R. P., Cornichet, J., and Iglesias Ponce de León, M.: Geochemical and geochronological cross section of the deep variscan crust: the Cabo Ortegal high-pressure nappe (NW Spain), in: *Terranes*

3566

- in the Variscan Belt of Europe and Circum-Atlantic Paleozoic Orogens: Tectonophysics, 177, edited by: Matte, P., Netherlands, Elsevier, 263–292, 1990.
- Pérez-Estaún, A., Martínez-Catalán, J. R., and Bastida, F.: Crustal thickening and deformation sequence in the footwall to the suture of the Variscan Belt of northwest Spain, Tectonophysics, 191, 243–253, 1991.
- 5 Platt, J. P.: Dynamics of orogenic wedges and the uplift of high-pressure metamorphic rocks, Geol. Soc. Am. Bull., 97, 1037–1053, 1986.
- Ponce, C., Druguet, E., and Carreras, J.: Development of shear zone-related lozenges in foliated rocks, J. Struct. Geol., 50, 176–186, doi:10.1016/j.jsg.2012.04.001, 2013.
- 10 Puellas, P., Ábalos, B., and Gil Ibarra, J. I.: Metamorphic evolution and thermobaric structure of the subduction-related Bacariza high-pressure granulite formation (Cabo Ortegal Complex, NW Spain), Lithos, 84, 125–149, doi:10.1016/j.lithos.2005.01.009, 2005.
- Ramsay, J. G.: Folding and Fracturing of Rocks, McGraw-Hill, New York, 568 pp., 1967.
- Ries, A. C. and Shackleton, R. M.: Catazonal complexes of northwest Spain and North Portugal, remnants of a Hercynian thrust plate, Nature, 234, 65–68, 1971.
- 15 Rubio-Ordóñez, A., Valverde-Vaquero, P., Corretge, L. G., Cuesta, A., Gallastegui, G., Fernández-Gonzalez, M., and Gerdes, A.: An early ordoevician tonalitic-granodioritic belt along the Schistose-Greywacke domain of the Central Iberian Zone (Iberian Massif, Variscan Belt), Geol. Mag., 149, 927–939, doi:10.1017/S0016756811001129, 2012.
- 20 Rutter, E. H., Mecklenburgh, J., and Brodie, K. H.: Rock mechanics constraints on mid-crustal low-viscosity flow beneath Tibet, in: Deformation Mechanisms, Rheology and Tectonics: Microstructures, Mechanics and Anisotropy, edited by: Prior, D. J., Rutter, E. H and Tatham, D. J., Geological Society of London Special Publications, 360, London, 329–336, doi:10.1144/SP360.19, 2011.
- 25 Santos-Zalduendo, J. F., Schaerer, U., Gil Ibarra, J. I., and Girardeau, J.: Origin and evolution of the Paleozoic Cabo Ortegal ultramafic-mafic complex (NW Spain); U-Pb, Rb-Sr and Pb-Pb isotope data, Chem. Geol., 129, 281–304, 1996.
- Shreve, R. L. and Cloos, M.: Dynamics of sediment subduction, melange formation, and prism accretion, J. Geophys. Res., 91, 10229–10245, 1986.
- 30 Stacey, J. S. and Kramers, J. D.: Approximation of terrestrial lead isotope evolution by a two-stage model, Earth Planet. Sc. Lett., 26, 207–221, 1975.
- Valverde, V. P. and Fernández, F. J.: Edad de enfriamiento U/Pb en rutilos del Gneiss de Chimparra (Cabo Ortegal, NO de España), Geogaceta, 20, 475–478, 1996.

3567

- Vera, J. A. (Ed.): Geología de España, SGE-IGME, Madrid, 2004.
- Vogel, D. E.: Petrology of an eclogite- and pyrigarnite-bearing polymetamorphic rock complex at Cabo Ortegal, NW Spain, Leidse Geologische Mededelingen, 40, 121–213, 1967.
- Whitney, D. L. and Evans, B. W.: Abbreviations for names of rock-forming minerals, Am. Mineral., 95, 185–187, 2010.
- 5

3568

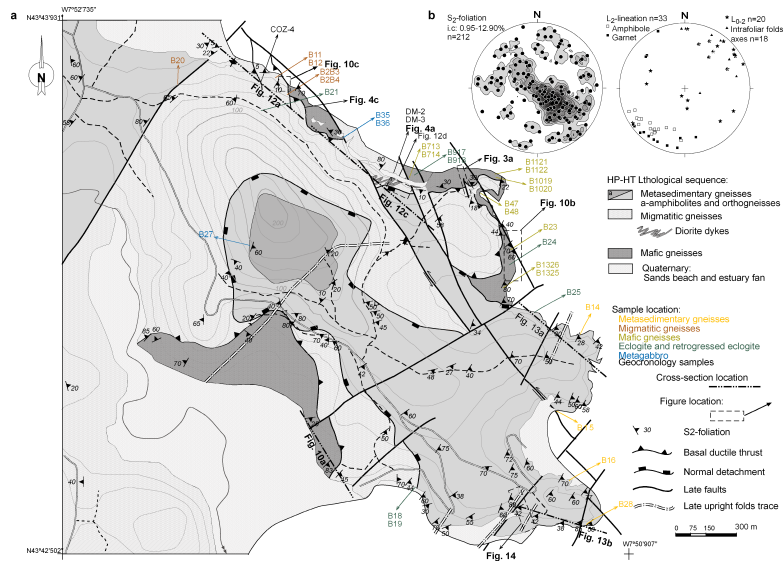


Figure 2. Geological map of the Masanteo peninsula with location of samples, figures and cross-sections (a). Pole figures in (b) show the distribution of S_2 foliation poles and related structures (lineation and intrafoliar fold axes). Equal area projection, lower hemisphere.

3571

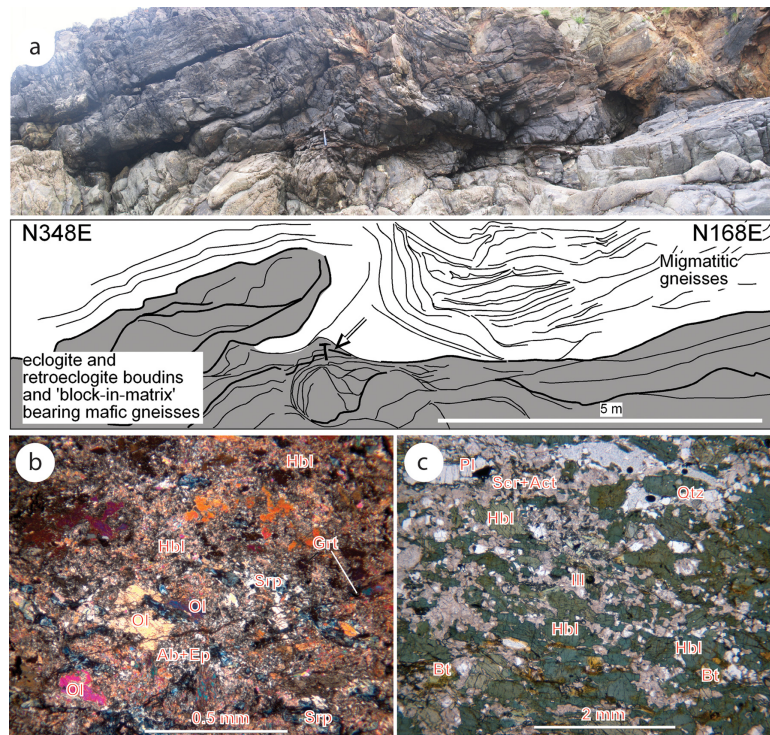


Figure 3. Mafic gneisses and related-rocks. (a) Structures at the outcrop scale, the sketch shows the attitude of the main S_2 foliation at the contact between mafic gneisses and migmatitic gneisses. Microphotographs: (b) retrogressed coronitic metagabbro (Sample B917). (c) Bt-Grt-bearing amphibolite gneisses within the less deformed lozenges (Sample B714). Sample location is indicated in Fig. 2a.

3572

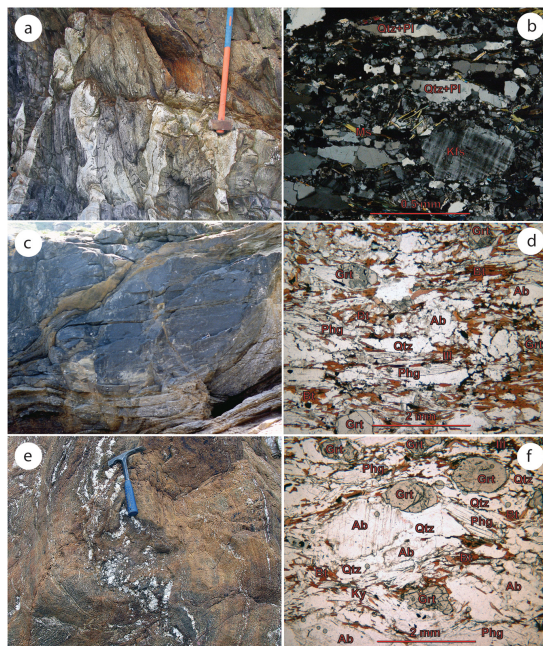


Figure 4. Migmatitic biotite Qz-Fsp gneisses and related-rocks. **(a)** Folding affecting a felsic dioritic dyke and the S_2 foliation. **(b)** Microphotograph of the felsic diorite dyke showing a coarse foliation (Sample DM-2). **(c)** Anastomosing shear zones defined by the S_2 foliation surrounding lozenges of less deformed migmatitic Qz-Fsp gneisses. **(d)** Microphotograph of the biotite Qz-Fsp gneisses (Sample B23). **(e)** Restite in migmatitic Qz-Fsp gneisses. **(f)** Microphotograph of the leucocratic Qz-Fsp gneisses (Sample B12). Sample locations are in Fig. 2a.

3573

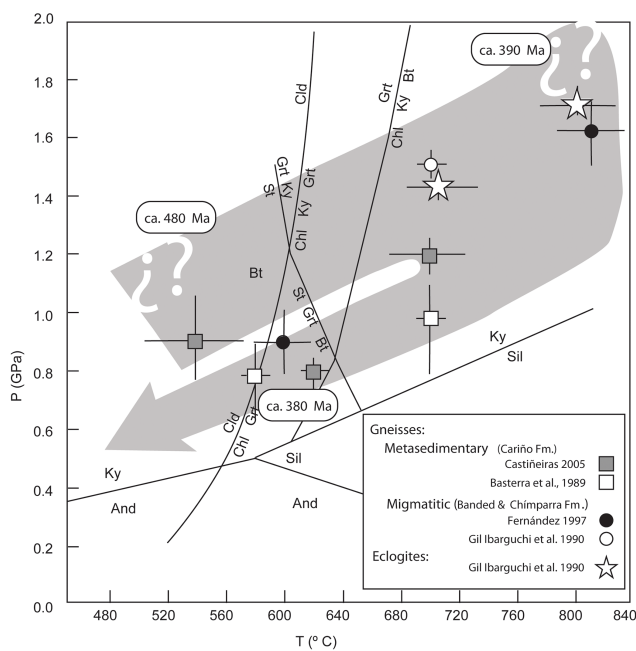


Figure 5. P - T data calculated for metasedimentary and migmatitic Qz-Fsp gneisses in Cabo Ortegal nappe, based in the available published data, indicated in the legend. Al_2SiO_5 phase diagram after Holdaway (1971). P - T path proposed (grey arrow) highlight with $\zeta?$ indeterminations in the prograde and maxima P - T boundaries of the migmatitic Qz-Fsp gneisses. The arrow in grey highlights the P - T - t evolution of metamorphic conditions just to the exhumation of Cabo Ortegal gneisses to amphibolite facies accordingly with our data.

3574

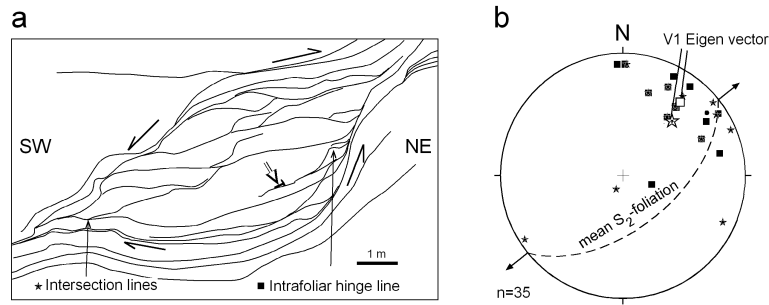


Figure 8. Relation of deformation structures inside and outside lozenge migmatitic bodies: **(a)** sketch showing the trace of the S₂ foliation in bounding shear zones and within the lozenge (location of observations in Fig. 4c); and **(b)** pole figure of main S₂ foliation, intersection lineation and intrafoliar hinge lines within the lozenge in **(a)**. Equal area projection, lower hemisphere projection also shows the V1 eigen vector and the mean S₂ foliation plane. The arrows indicate the orientation of the horizontal maximum extension inferred.

3577

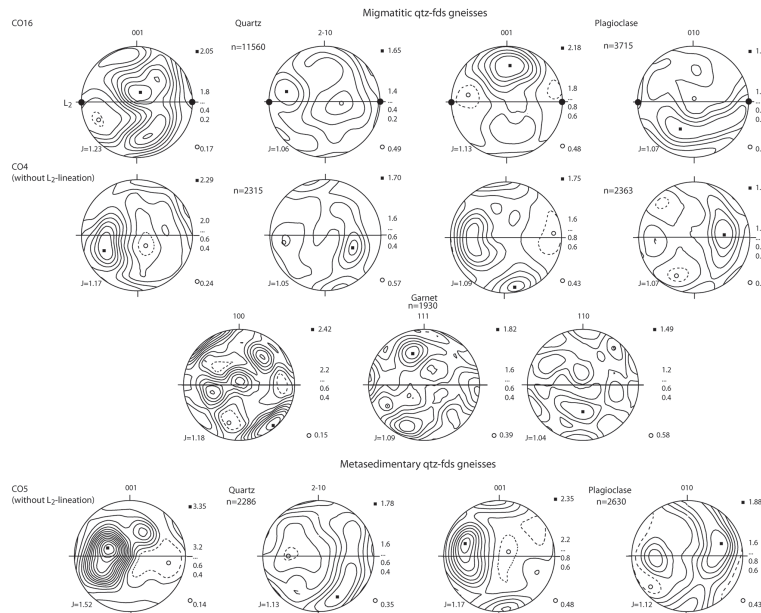


Figure 9. Crystallographic preferred orientation (CPO) patterns in quartz and plagioclase, in relation to the main S₂ foliation in the Qz-Fsp gneisses. Sample locations are in Fig. 2. Contouring is in multiples of random distribution (gaussian halfwidth 15). Items indicated in the stereonets are: bottom left, the J index; right, the values of contours. Equal area projection, lower hemisphere. S₂ foliation is plotted E-W vertical and the L₂ lineation, if sufficiently developed, is plotted E-W horizontal. Crystallographic preferred orientation (CPO) pattern in garnet formed in the S₂ tectonic fabric in sample CO4 is also plotted.

3578

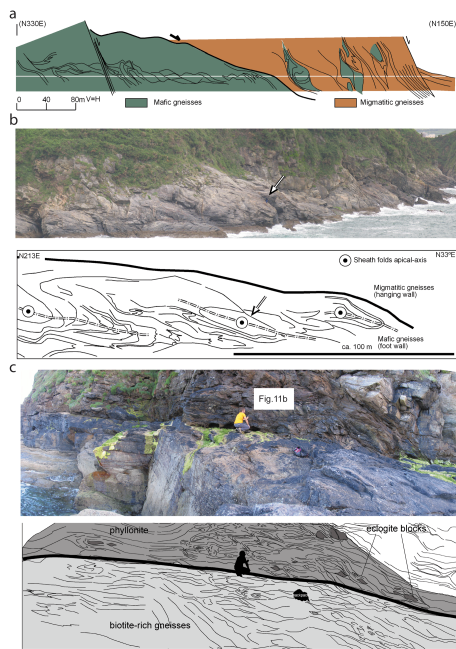


Figure 10. Coastal sections of the basal thrust (see Figs. 2a and 12a for locations). **(a)** Continuous section showing the contact between the mafic gneisses and the migmatitic gneisses. The white line represents the sea level. **(b)** Elliptical sections in sheath folds of decametric size in the lower domain of the basal thrust. The arrow points to an angle for scale, also used as reference in the sketch outlining the S_2 foliation underneath. **(c)** Phyllonitic domain in the basal thrust. Structures related to this domain are outlined in the sketch below the picture.

3579

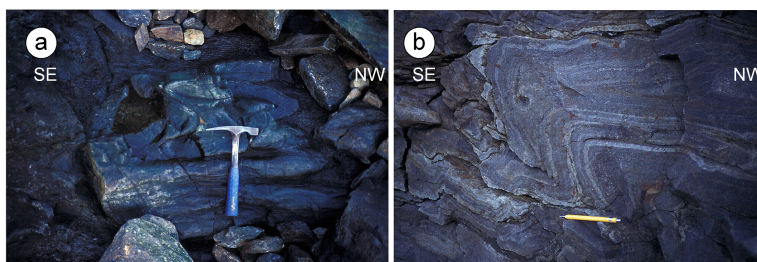


Figure 11. Non-cylindrical minor fold associated to the basal thrust: **(a)** sheath folds with apical axes perpendicular to the section view; and **(b)** type 3 fold interference pattern (after Ramsay, 1967) in the phyllonitic domain (see Fig. 10 for location).

3580

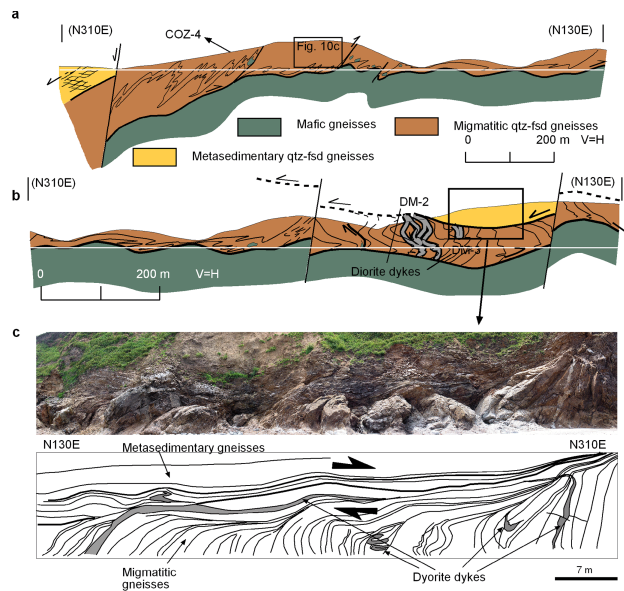


Figure 12. Geological sections showing the internal structure of the migmatitic Qz-Fsp gneisses and the locations of larger eclogite-blocks. Cross sections are located in Fig. 2a. The white lines represent the sea level. **(a)** In the northern section, the internal structure is characterized by asymmetrical folding and the presence of eclogite block-in-matrix close to the thrust. **(b)** The internal structure of the migmatitic Qz-Fsp gneisses is dominated by the presence of polyclinal folds bounded by the basal thrust and the upper normal detachment. **(c)** Photograph and sketch in the cliff of the Serrón beach showing a normal detachment placing the metasedimentary gneisses on top of the migmatitic gneisses. Location of the sections is in Fig. 2a.

3581

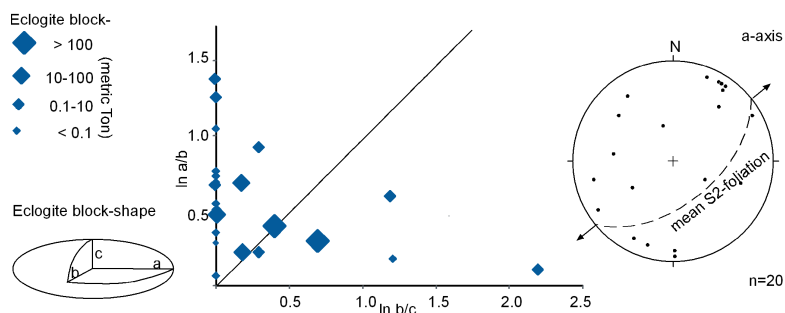


Figure 13. The shape of the eclogite block-in-matrix show a range of geometries in a Flinn diagram from prolate to oblate. The size of the symbols is proportional to size of the blocks. The scattering of the major axes of eclogite block-in-matrix in a lower hemisphere equal area projection is consistent with an overall flattening strain geometry for the unit.

3582

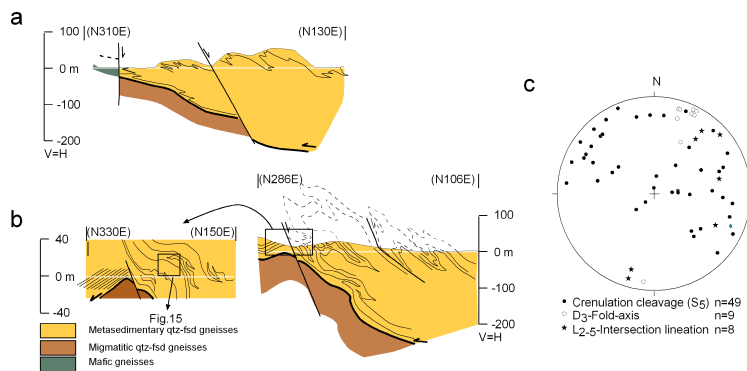


Figure 14. Geological sections of the D_3 recumbent syncline reconstructed from the small-scale parasitic folds that are folding the main S_2 foliation. Location of the sections is in Fig. 2a. White lines represent the sea level. **(a)** Northern outcrop-section. **(b)** Southern outcrop-section and the structural detail with location of Fig. 15. Note that the recumbent synform is affected by open-upright D_5 folds. **(c)** Crenulation cleavage S_5 , D_3 fold axes and L_{2-5} intersection lineation is plotted in an equal area, lower hemisphere projection.

3583

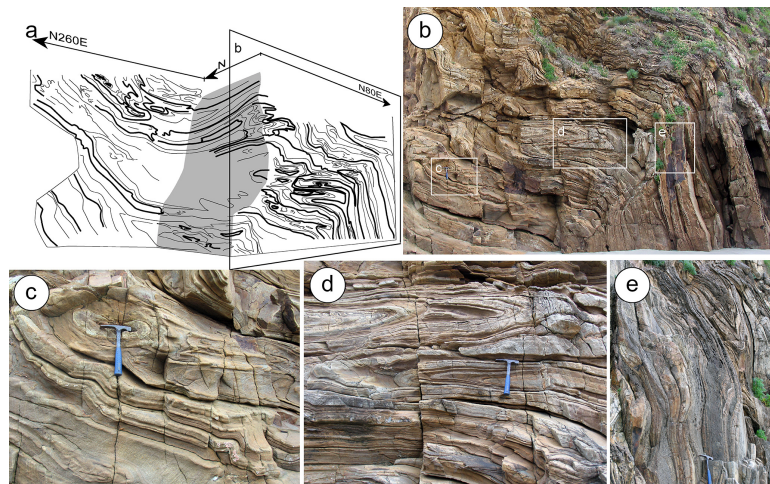
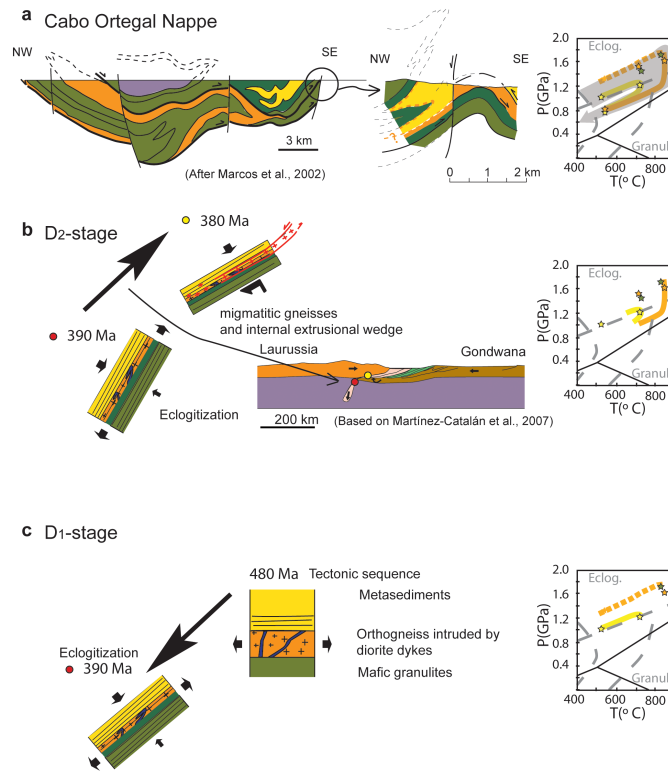


Figure 15. Small-scale parasitic folds related to the recumbent synform folding prior to D_2 isoclinal folds. Locations of outcrops are indicated in Figs. 3 and 14. **(a)** Sketch of the outcrop-section. **(b)** W-E view of a monocline, with location of the photographs **(c)**, **(d)** and **(e)**. **(c)** The apical-section of a D_2 sheath-fold, behind the hammer, indicates a N-S stretching direction. **(d)** D_2 intrafoliar folds folded by a "Z" parasitic D_3 fold (reverse limb of the D_3 recumbent fold). **(e)** "Z" parasitic D_3 fold rotated by the D_5 monocline.

3584



3585

Figure 16. Synthetic evolution of the high-grade deformed qzt-fds gneisses of the Cabo Ortegal Nappe. **(a)** Simplified geological section of the Cabo Ortegal nappe at present, showing the detail of the structure in the Masanteo peninsula (cross section in Fig. 1d, modified from Marcos et al., 2002). The P - T path to the right is based on Fig. 5. Note that coordinates correspond to present and the superposed structures from the second phase of deformation correspond to the exhumation and accretion of the Cabo Ortegal nappe onto the Iberian plate. **(b)** D_2 stage (From 390 to 380 Ma) highlighting the effect of the eclogitization after the slab breakoff, increasing the rheological contrast between the migmatized Qz-Fsp gneisses, the eclogites and the top of the Qz-Fsp gneisses during the development of the main blastomylonitic foliation. The P - T diagram is showing the convergence of P - T paths by the migmatitic and the metasedimentary Qz-Fsp gneisses during this stage. The tectonic sketch showing the collision between Laurentia and the northern margin of Gondwana since Middle Devonian (390 Ma) and Upper Devonian (380 Ma) is based on Martínez-Catalán et al., 2007. Red and yellow points indicate the inferred location of the tectonic sequence. **(c)** Two partial melting events are reported, the first at high-pressure granulite facies conditions in mafic rocks (490 Ma) led to the intrusion of dioritic dykes in the Qz-Fsp gneisses. The second subsequent to Variscan eclogitization at 390 Ma. Arrows propose the finite strain orientation.

3586